# Summer transport estimates of the Kamchatka Current derived as a variational inverse of hydrophysical and surface drifter data

G. G. Panteleev,[1,2] P. Stabeno,[3] V. A. Luchin,[4] D. A. Nechaev,[5] and M. Ikeda[6]

Received 23 October 2005; revised 21 December 2005; accepted 30 December 2005; published XX Month 2006.

[1] The quasistationary summer Bering Sea circulation is reconstructed as a variational inverse of the hydrographic and atmospheric climatologies, transport estimates through the Bering Strait, and surface drifter data. Our results indicate the splitting of the Kamchatka Current in the vicinity of the Shirshov Ridge. This branching is in agreement with independent ARGO drifter observations. It was also found, that transport of the Kamchatka Current gradually increases downstream from 14 Sv in the Olyutorsky Gulf to 24 Sv in the Kamchatka Strait, which is twice higher than previous estimates. **Citation:** Panteleev, G. G., P. Stabeno, V. A. Luchin, D. A. Nechaev, and M. Ikeda (2006), Summer transport estimates of the Kamchatka Current derived as a variational inverse of hydrophysical and surface drifter data, *Geophys. Res. Lett.*, *33*, LXXXXX, doi:10.1029/2005GL024974.

## 1. Introduction

[2] The circulation and distributions of the hydrophysical properties in the Bering Sea (BS) determine the heat and fresh water exchange between the North Pacific and Arctic Oceans. The circulation in the BS basin is driven by the atmospheric forcing and the inflow/outflow transports through four primary passes: Kamchatka Strait, Near Strait, Amchitka Pass and Amukta Pass [*Stabeno et al.*, 2005]. The currents in the Bering Strait are relatively well monitored by velocity moorings [*Woodgate et al.*, 2005], while the water transports through the straits and passages of the Aleutian Arc have been mainly explored through the estimates of the baroclinic currents by dynamical method [*Verhunov and Tkachenko*, 1992; *Stabeno and Reed*, 1992]. The transport through the Kamchatka Strait is the major outflow from the BS. This region is one of the least studied in the BS because of known difficulties in accessing the Russian historical data. The estimates of the Kamchatka Current (KC) transport are based mainly on the hydrophysical data and range from 5 Sv [*Verkhunov and Tkachenko*, 1992] to 15 Sv [*Ohtani*, 1970] in dynamical calculations and 8–13 Sv in numerical modelling studies [*Overland et al.*, 1994]. Unfortunately, the results of both these methods depend on a number unknown parameters, such as the level of no motion or poorly known boundary conditions and tidal rectification through many of the passes that are often not resolved in models [*Stabeno et al.*, 2005].

[3] The goal of this study is to quantify the summer circulation in the central BS and to derive reliable estimates of the KC transport by combining the information from all available data sources with the dynamical constraints of the primitive equation numerical model. We solve this problem through the variational assimilation of temperature/salinity, drifter and meteorological data into the ocean general circulation model [*Nechaev et al.*, 2005; *Panteleev et al.*, 2006]. The summer period was chosen as the period with the best data coverage.

## 2. Data

[4] In the presented research we utilize data sets as follows.

### 2.1. 41,911 Temperature/Salinity Profiles Collected in the Chukcha and Bering Seas (Between 55°N and 69°N) During the Summer (July–September)

[5] This database includes bottle data, mechanical bathythermograph data, high resolution CTD, expendable bathythermograph and PALACE ARGO drifter data. The data were collected by US, Japanese and Russian organizations during the period 1932–2004. The major part of the data was obtained from historical databases in RIHMI-WDC (http://www.meteo.ru/nodc/), JODC (http://jdoss1.jodc.go.jp), University of Alaska (http://www.ims.uaf.edu), databases of Levitus [*Levitus et al.*, 2001], and Argo Global Data Assembly Centre (http://www.coriolis.eu.org//cdc/argo.htm). Some of Russian data are classified and not available to the public at present. Figure 1 shows the spatial distribution of salinity profiles. These climatological data and estimates of their standard deviation (STD) were used in data assimilation. Temperature/salinity STD varied within the ranges 0.5°C–1.5°C and 0.1–2.0 near the surface and decreased down to 0.1°C and 0.03 respectively on deeper levels (1000 m).

### 2.2. 500 Satellite-Tracked Drifters Trajectories From Fisheries Oceanography Coordinated Investigations (NOAA) Database (http://www.pmel.noaa.gov/foci/FOCI_data.html)

[6] All surface drifters utilized in this paper had drougues at approximately 40 m [e.g., *Stabeno and Reed*, 1994]. The preliminary analysis of these data included: (i) extraction of summer drifter trajectories; (ii) temporal low-pass filtering with a 7 days cutoff period; (iii) spatial interpolation and smoothing of the filtered drifter velocity components onto

[1]International Arctic Research Center, University of Alaska Fairbanks, Fairbanks, Alaska, USA.
[2]Also at Shirshov Institute of Oceanology, Russian Academy of Sciences, Moscow, Russia.
[3]Pacific Marine Environmental Laboratory, Seattle, Washington, USA.
[4]Il'ichev Pacific Oceanological Institute, Far Eastern Branch, Russian Academy of Science, Vladivostok, Russia.
[5]Department of Marine Science, University of Southern Mississippi, Stennis Space Center, Mississippi, USA.
[6]Graduate School of Environmental Earth Science, Hokkaido University, Sapporo, Japan.


0094-8276/06/2005GL024974$05.00

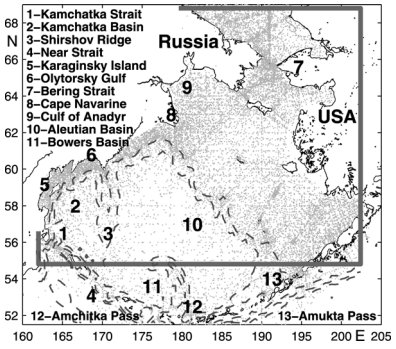


**Figure 1.** Spatial distribution of the summer historical salinity data in the Bering Sea. The model domain is shown by thick line. Dashed lines mark the 1000 m and 3000 m isobaths.

the model grid with correlation radius of 40 km; (iv) estimation of the error variance of gridded velocity components. We assimilated only ''reliable'' velocities obtained from the averaging of at least three different surface drifters (Figure 2).

### 2.3. Estimates of the Total Summer Transports Through the Bering Strait

[7] Transport estimates of 1.1 ± 0.2 Sv were taken from [*Woodgate et al.*, 2005].

### 2.4. NCEP/NCAR Wind Stress and Surface Heat/Salt Flux Climatology

[8] These climatologies (http://www.cdc.noaa.gov/cdc/data.ncep.reanalysis.derived.html) were found to be extremely smooth. To allow for the adjustment of the spatial details in the model forcing we used wind stress and heat/salt flux data with relatively high error variance equal to 40% of their spatial and temporal variability in the BS. Significant errors in the NCEP/NCAR forcing were also noticed by *Ladd and Bond* [2002].

## 3. Data Assimilation Technique

[9] To find the optimal solution of the model we perform strong constraints minimization of the cost function measuring the distance between the model solution and data on the space of the control variables [*Le Dimet and Talagrand*, 1986]. Control variables include the initial conditions, the model field values required to specify the open boundary conditions, and the surface fluxes of momentum, heat and salt [*Nechaev et al.*, 2005].

[10] The primitive equation model utilized in this study was successfully used for the reconstruction of the climatological circulation in the Barents Sea [*Panteleev et al.*, 2006] and for the nowcast of the circulation in the Tsushima Strait [*Nechaev et al.*, 2005]. The model is a modification of the C-grid, *z*-coordinate OGCM designed by *Madec et al.* [1999]. The model is implicit both for barotropic and baroclinic modes permitting model runs with relatively large time steps [*Nechaev et al.*, 2005]. The model is configured in the domain shown in Figure 1 and is used in ''climatological'', ''quasistationary'' [*Tziperman and Thacker*, 1989] non-eddy-resolving mode on a relatively coarse regular z-coordinate grid. The meridional resolution of the grid is 0.2°, zonal resolution – 0.4°, and the time step is 4 hours. Vertically the grid has 34 levels with unequal spacing ranging from 5 m at the surface to 500 m in the deeper levels. The smaller passes in the Aleutian Arc are not resolved, but the primary ones are.

[11] Statistical interpretation of the variational data assimilation technique [*Thacker*, 1989] considers the cost function as an argument of the Gaussian probability distribution with the cost function weights being the inverse covariances of the corresponding data errors. In the present study we use the cost function $\mathcal{J}$ containing ''data'', ''smoothness'' and ''stationarity'' terms:

$$\mathcal{J} = \mathcal{J}_{data} + \mathcal{J}_{smoth} + \mathcal{J}_{stat}, \quad \text{where}$$

$$\mathcal{J}_{data} = W_y^{-1}(y - y^*)^2 + W_Y^{-1}(Ly - Y^*)^2,$$

$$\mathcal{J}_{smoth} = \int_{\Omega,t} W_{y,s}^{-1}\left(\nabla^2 y\right)^2 d\Omega dt, \tag{1}$$

$$\mathcal{J}_{stat} = \int_{\Omega,t} W_{y,t_1}^{-1}(\partial y/\partial t)^2 + W_{y,t_2}^{-1}\left(\partial^2 y/\partial t^2\right)^2 d\Omega dt.$$

[12] Here Ω is the model domain; $y$ stands for the vector of the model solution, and $y^*$ – for the corresponding gridded data; $Y^*$ denotes the data, which are not direct measurement of the model state vector and require some

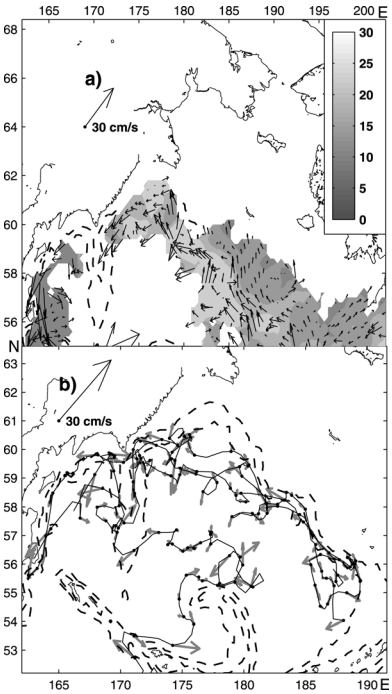


**Figure 2.** (a) Averaged summer velocities at 40 m derived from drifter data. The shaded areas show the spatial distribution of zonal velocity STD, which ranges from 5 cm/sec to 20 cm/sec. (b) The trajectories and 2-day mean velocities of the four ARGO drifters (http://www.usgodae.org) parked at 1000 m during 2002–2004. Circles and asterisks designate the initial and final location of the drifter. Dashed lines denote 1000 m and 3000 m isobath.

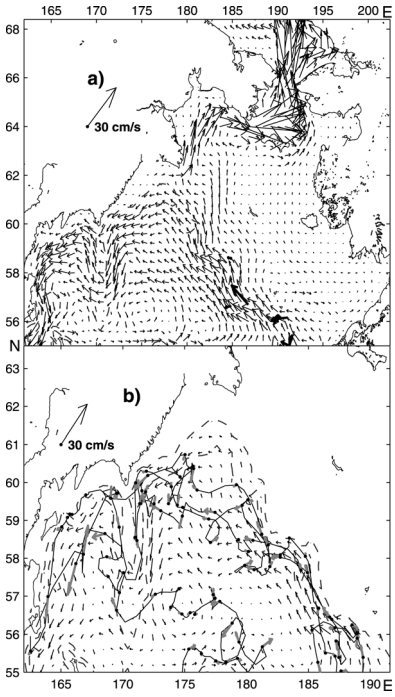


**Figure 3.** The optimized velocities at (a) 17 m and (b) 1000 m obtained in the experiment A. Thick arrows denote the mean velocities observed at several moorings (Figure 3a) and ARGO velocities at 1000 m (Figure 3b).

operator $L$ acting on the model solution $y$ to compute model-data counterparts (e.g., $L$ can calculate the transports through the open boundaries). The diagonal matrices $W_y$, $W_Y$, $W_{y,s}$ are the variances of the corresponding data and smoothness terms (see Data section).

[13] In the course of $\mathcal{J}$ minimization, the term $\mathcal{J}_{data}$ forces the model solution to be close to the data, the term $\mathcal{J}_{smoth}$ penalizes grid-scale noise. The "stationarity" cost function term $\mathcal{J}_{stat}$ allows us to obtain a quasi-steady state model solution [*Tziperman and Thacker*, 1989] and to find the estimates of the summer climatological state. The weights $W_{y,t_1}$ and $W_{y,t_2}$ define "degree" of stationarity of model solution. The climatological temperature/salinity distributions and the corresponding geostrophic velocities were used to set up boundary and initial conditions for the first guess solution of the model.

## 4. Results

[14] The reconstruction of the climatological summer circulation was done using quasistationary variational data assimilation approach proposed by *Tziperman and Thacker* [1989]. We carried out two numerical experiments:

[15] Experiment A: we assimilated all the observations outlined above, i.e., temperature and salinity climatologies, surface drifter data, the Bering Strait transport, and meteorological data.

[16] Experiment B: we did not assimilate the surface drifter data, but instead, we added to the cost function the transport estimate of 12 ± 4 Sv through the Kamchatka Strait. This outflow estimate is derived from a number of publications implementing the dynamical method calculations [e.g., *Stabeno and Reed*, 1992; *Verhunov and Tkachenko*, 1994].

### 4.1. Experiment A

[17] The optimized velocity fields obtained in experiment A are shown in Figure 3. General circulation pattern agrees with conventional scheme of the BS circulation, which includes week currents on the eastern shelf, the Bering Slope current (BSC), the intensive KC along the Eurasian continent, the intensive Navarine Current in the Gulf of Anadir and the strong northward flow in the Bering Strait. The KC originates as a continuation of the BSC at approximately 175° and then flows clockwise around the Shirshov Ridge. The obtained circulation reveals strong topographic steering of the KC. According to our results, in the vicinity of the point 58°N, 170°E the KC splits into two branches. One of these branches (we will call it "coastal branch") follows northward along the 1000 m isobath, while, the other branch ("off-shore branch") flows westward across the Kamchatka Basin and joins the coastal branch of the KC near the Karaginsky Island. This is similar to the flow pattern by *Stabeno and Reed* [1994]. These branches join northeast of the Karaginsky Island resulting in the gradual increase of the KC transport from approximately 14 Sv in the Olyutorski Gulf to 24 Sv in the Kamchatka Strait. The obtained estimate of the KC transport is almost 1.5–2 times higher than the "traditional" estimates derived by dynamical method.

[18] The mean relative error between modeled surface velocities (Figure 3a) and drifter velocities (Figure 2a) is 0.71. This relatively high error can be explained by the high STD of drifter velocities, which reaches 20 cm/s in the BSC (Figure 2a). Despite the high error, the absolute amplitude of the surface velocities in Bering Slope and Kamchatka Currents (Figure 3a) are close to the amplitude of drifter velocities shown in Figure 2a. A limited amount of available mooring velocities (Figure 3a, thick arrows) reveals very good agreement with optimized velocities. Unfortunately, most of these data are located in the eastern part of the BS and cannot confirm the reliability of the KC reconstruction. Because of that, we compare our results with the trajectories of four ARGO drifters (www.usgodae.org), which were launched at 1000 m depth.

[19] Three of these drifters were released in the southeastern part of the BS and were carried by the BSC up to 58°–59°N where they deflected from the continental slope and drifted across the Aleutian Basin to the Shirshov Ridge, where they joined KC. One of these drifters entered the KC and sailed clockwise around the Shirshov Ridge up to 60°N; that is, the trajectory of this drifter follows the "coastal" branch of the KC discussed above (Figures 3a and 3b). The fourth drifter entered the BS through the Near Strait (Figure 2b). The drifter crossed the Bowers and Aleutian Basins and joined the KC near the southern end of the Shirshov Ridge (Figure 3b) and drifted clockwise around the ridge. This drifter deflected westward at 58°N, 170°E following the "off-shore" branch of the KC obtained in our results. The splitting of the KC at this point is probably caused by sharp bottom topography changes in the Shirshov Ridge region. Analysis of bottom relief (Figure 1) allows us to speculate, that off-shore branch initially follows the 3000 m isobath and then deflects

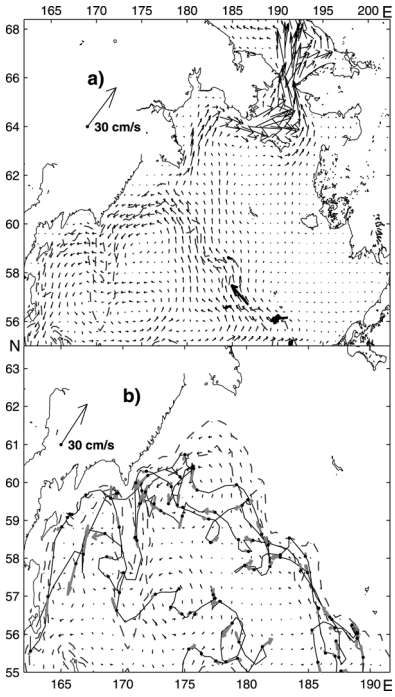


**Figure 4.** The optimized velocities at (a) 17 m and (b) 1000 m obtained in the experiment B. Thick arrows denote the mean velocities observed at several moorings (Figure 4a) and ARGO velocities at 1000 m (Figure 4b).

westward near 58°N, 170°E, while the trajectory of the coastal branch of the KC coincide with the 1000 m isobath.

[20] The 2-day mean velocities of the ARGO drifters are shown in Figure 2b. The averaged speed of these four drifters was approximately 4.5 cm/sec. This value is close to the mean 3.5 cm/sec speed of the modeled currents at 1000 m (Figure 3b). That seems to be a good agreement with observations, because Lagrangian velocity estimates tend to be larger than Eulerian.

### 4.2. Experiment B

[21] Velocity field obtained in experiment B are shown in Figure 4. The solution without drifter data assimilation retains most of the features of the BS circulation [*Stabeno and Reed*, 1994] and visually the circulation pattern is similar to the circulation in Figure 3. Meanwhile, the detailed analysis reveals both qualitative and quantitative differences.

[22] For example, the BSC in the experiment B does not deflect westward in the vicinity of 59°N and continues to follow the slope up to 62°N. That contradicts to the trajectories of all ARGO drifters in this region (Figures 2b and 4b). Both surface and deep velocities in Figure 4 do not reveal "branching" of the KC on the western slope of the Shirshov Ridge (58°N, 170°E), which is supported by ARGO drifters trajectories.

[23] The quantitative analysis of the velocity fields reveals even stronger difference between velocities in Figure 4 and observations. On the level of 1000 m, the averaged speed in the experiment B (Figure 4b) is approximately 1.5 cm/s, which is more than two times smaller than the velocities in the experiment A (3.3 cm/s) and three times smaller than the observations of ARGO floats (4.5 cm/s). Similar differences can be observed in the surface layer: the surface velocities in the experiment B in the vicinity of Kamchatka Strait is only about 5 cm/sec, while the drifters give the averaged estimate of 20–30 cm/s. Overall we can state, that the velocity field obtained in the experiment B only approximately agrees with the available velocity observations.

## 5. Conclusions

[24] The performed numerical experiments and comparison with surface and ARGO drifters reveal the splitting of the BSC in the vicinity of 58°N 180°E and KC on the western slope of the Shirshov Ridge and indicate that traditional transport estimate of 12 Sv through the Kamchatka Strait is not a realistic climatological estimate. The most probable climatological summer state (experiment A) derived from the assimilation of all available data [*Thacker*, 1989] shows that the transport of the KC increases gradually from 14 Sv in the Olyutorsky Gulf to 24 Sv in the Kamchatka Strait. Our KC transport estimate is in a good agreement with the 20 Sv summer KC transport obtained by combining the section hydrophysical data and surface floats data by *Hughes et al.* [1974]. Also, higher than traditional transport estimates has been obtained recently by *Stabeno et al.* [2005]. This paper provides the analysis of the direct velocity measurements and derives the inflow estimate into the Bering Sea of 4 Sv through the Amutka Pass, which is five times higher than the previous estimates.

[25] We speculate that the difference between the traditional transport estimates and the results of the present study can be explained by some underestimation of the barotropic velocity component in the Bering Sea in the traditional transport estimates. To support this speculation we calculated baroclinic transport through the Kamchatka Strait by dynamical method with zero bottom velocities from hydrographic data utilized in the paper. Our estimate of the baroclinic transport of approximately 10 Sv appeared to be very close to the traditional transport estimates cited in the literature [*Ohtani*, 1970; *Verhunov and Tkachenko*, 1994].

[26] Due to the model limitations the study region does not extend south of 55°N. In the future we plan to apply similar technique for the reconstruction of BS circulation within it's natural boundaries (Aleutian Arc and Bering Strait) and to provide comprehensive analysis of the temperature/salinity distributions and posterior error analysis.

[27] **Acknowledgments.** This study was funded by the FRSGC, through JAMSTEC, Japan, and sponsorship of IARC. The study was supported by the ONR Grant N00014-00-1-0201, NSF Grant OCE-01-18200 and RFFI Grant 06-05-96065. This is also contribution 2873 to PMEL.

## References

Hughes, F. W., L. K. Coachman, and K. Aahaard (1974). Circulation, transport and water exchange in the western Bering Sea, in *Oceanography of the Bering Sea With Emphasis on Renewable Resources*, edited by D. W. Hood and E. J. Kelley, pp. 59–98, Inst. of Mar. Sci., Univ. of Alaska Fairbanks, Fairbanks.

Ladd, C., and N. Bond (2002), Evaluation of the NCEP/NCAR reanalysis in the NE Pacific and at the Bering Sea, *J. Geophys. Res.*, *107*(C10), 3158, doi:10.1029/2001JC001157.

Le Dimet, F. X., and O. Talagrand (1986), Variational algorithms for analysis and assimilation of meteorological observations: Theoretical aspects, *Tellus, Ser. A*, *38*, 97–100.

Levitus, S., et al. (2001), *World Ocean Database* [CD-ROM], Natl. Oceanogr. Data Cent., Silver Spring, Md.

Madec, G., P. Delecluse, M. Imbard, and C. Levy (1999), *OPA8.1 Ocean General Circulation Model Reference Manual*, *Notes Pole Model.*, vol. 11, 91 pp., Inst. Pierre-Simon Laplace, Paris.

Nechaev, D., G. Panteleev, and M. Yaremchuk (2005), Reconstruction of the circulation in the limited region with open boundaries: Circulation in the Tsushima Strait, *Okeanologiya*, *45*, 805–828.

Ohtani, K. (1970), Relative transport in the Alaskan Stream in winter, *J. Oceanogr. Soc. Jpn.*, *26*, 271–282.

Overland, J. E., M. C. Spillane, H. E. Hurlburt, and A. J. Wallcraft (1994), A numerical study of the circulation of the Bering Sea basin and exchange with the North Pacific Ocean, *J. Phys. Oceanogr.*, *93*, 15,619–15,637.

Panteleev, G., D. Nechaev, and M. Ikeda (2006), Reconstruction of summer Barents Sea circulation from climatological data, *Atmosphere Ocean*, in press.

Stabeno, P. J., and R. K. Reed (1992), A major circulation anomaly in the western Bering Sea, *Geophys. Res. Lett.*, *19*, 1671–1674.

Stabeno, P. J., and R. K. Reed (1994), Circulation in the Bering Sea basin observed by satellite-tracked drifters: 1986–1993, *J. Phys. Oceanogr.*, *24*, 848–854.

Stabeno, P. J., D. G. Kachel, and M. E. Sullivan (2005), Observation from moorings in the Aleutian Passes: Temperature, salinity and transport, *Fish. Oceanogr.*, *14*, suppl. 1, 39–54.

Thacker, W. C. (1989), The role of the Hessian matrix in fitting models to measurements, *J. Geophys. Res.*, *94*, 6177–6196.

Tziperman, E., and W. C. Thacker (1989), An optimal-control/adjoint equation approach to studying the oceanic general circulation, *J. Phys. Oceanogr.*, *19*, 1471–1485.

Verhunov, A. V., and Y. Y. Tkachenko (1994), Recent observations of variability in the western Bering Sea current system, *J. Geophys. Res.*, *97*, 14,369–14,376.

Woodgate, R. A., K. Aagaard, and T. J. Weingartner (2005), Monthly temperature, salinity, and transport variability of the Bering Strait through flow, *Geophys. Res. Lett.*, *32*, L04601, doi:10.1029/2004GL021880.

M. Ikeda, Graduate School of Environmental Earth Science, Hokkaido University, Sapporo 060-0810, Japan.

V. A. Luchin, Il'ichev Pacific Oceanological Institute, Far Eastern Branch, Russian Academy of Science, Vladivostok 690041, Russia.

D. A. Nechaev, Department of Marine Science, University of Southern Mississippi, Stennis Space Center, MS 39529–9904, USA.

G. G. Panteleev, International Arctic Research Center, University of Alaska Fairbanks, Fairbanks, AK 99775–7335, USA. (gleb@iarc.uaf.edu)

P. Stabeno, Pacific Marine Environmental Laboratory, Seattle, WA 98115–6349, USA.